PHYSICAL REVIEW B VOLUME 10, NUMBER 5 1 SEPTEMBER 1974

Neutron-scattering studies of spin waves in rare-earth orthoferrites

S. M. Shapiro and J. D. Axe
Physics Department, Brookhaven National Laboratory, Upton, New York 11973*

J. P. Remeika
Bell Laboratories, Murray Hill, New Jersey 07974

(Received 14 May 1974)

Iron sublattice spin waves have been studied in $TmFeO_3$ and $ErFeO_3$ by inelastic neutron scattering. In $TmFeO_3$ magnon dispersion curves were measured along several symmetry directions and the results fitted to an isotropic Heisenberg Hamiltonian with near-neighbor exchange constant $J = (-29.1 \pm 0.6)$°K and next-nearest-neighbor exchange $J' = (-1.9 \pm 0.2)$°K. A detailed high-resolution study of the long-wavelength spin waves was performed near the moment reorientation transformation. In $TmFeO_3$, the lowest magnon frequency renormalizes in qualitative agreement with the "soft"-mode theory of the transformation. In $ErFeO_3$ mode softening was observed only at the lower transformation temperature. Improved estimates are made of the twofold and fourfold anisotropy energies in $TmFeO_3$.

I. INTRODUCTION

Rare-earth orthoferrites exhibit a number of intriguing magnetic properties.[1] Most notable is the weak ferromagnetism observed as a result of the canted antiferromagnetic ordering of the iron moments. Because of the large anisotropy associated with this small magnetic moment, the orthoferrites are the prototype materials for magnetic "bubble" devices. Other materials have since replaced orthoferrites in bubble technology but there still remain many interesting problems in understanding the magnetic interactions in the orthoferrites. Particularly intriguing is the existence in certain rare-earth orthoferrites of spin-reorientation transformations, in which the ordered spins rotate with respect to the crystal axes. It is thought that these spin-reorientation transformations are driven by soft spin-wave modes quite analogous to certain structural phase transformations which are known to result from unstable phonon modes, and which have been extensively studied by inelastic-neutron-scattering experiments.[2]

The rare-earth orthoferrites (RE FeO_3) crystallize in an orthorhombically distorted perovskite structure with four molecular units per unit cell and having a space-group symmetry D_{2h}^{16}-$Pbnm$.[3,4] The iron moments order antiferromagnetically at temperatures between 600 and 700 °K in all the RE FeO_3 compounds[1] and, since the ordering of the rare earths, if they do indeed order,[5] occurs at low temperatures ($T \sim 5$ °K)[4] we shall be concerned only with the magnetic interactions of the iron sublattices. Figure 1 shows the iron atoms in the unit cell which are located in the octahedral positions of the undistorted cubic perovskite structures. The + and − signs refer to the relative direction of the spins. In this G-type configuration,[6] each iron atom has six near neighbors (nn) with oppositely directed spins and the 12 next-near neighbors (nnn) with spins parallel, and results from the strong antiferromagnetic coupling between nearest-neighbor Fe sublattices. There is, in addition, a weak antisymmetric exchange coupling[7,8] which causes a canting of the spins on different sublattices. Of the possible resulting spin configurations compatible with crystallographic symmetry we are concerned with two,[1] shown schematically in Fig. 2. The first (G_x) consists of a G-type antiferromagnetic arrangement with spins slightly canted from the $\pm x$ axes, whereas in the second (G_z), the spins lie nearly along the $\pm z$ axes. The G_x configuration is the energetically favored one at high temperatures for all of the RE FeO_3 family. There are, however, temperature-dependent changes in the single-ion anisotropy, which seem to arise indirectly from induced RE ion polarization, which may favor the G_z configuration at lower temperatures. Such spin-reorientation transformations occur in Sm, Tb, Er, and Tm orthoferrites[1] and have two characteristic temperatures, an upper temperature T_u, at which the spins begin to rotate away from the $\pm x$ direction and a lower one T_l, at which the rotation is completed and the spins lie along $\pm z$. The rotation is confined to the xz plane by virtue of the antisymmetric exchange coupling. The equilibrium configuration in the reorientation region has been studied by magnetic-torque measurements,[9,10] Mössbauer effect,[11,12] optical measurements,[13–15] and elastic neutron scattering.[5,16] The dynamics of the reorientation process have been probed by microwave resonance[17] and indirectly by ultrasound propagation.[18] The advantage of inelastic neutron scattering over these latter techniques is the ability to couple directly to antiferromagnetic fluctuations.

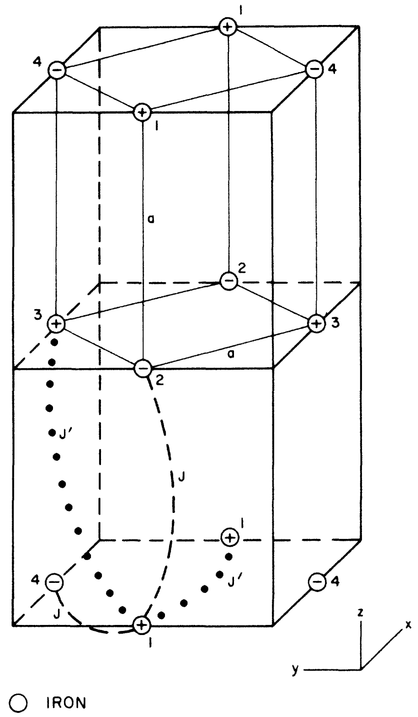

FIG. 1. Unit cell of RE FeO_3, symmetry D_{2h}^{16}-*Pbnm*, showing only the positions of the iron atoms. The relative direction of the spins is represented by the + and − signs. *J* and *J*′ are the nn and nnn exchange.

To interpret the neutron-scattering results to follow we adopt the following Hamiltonian[19]:

$$\mathcal{H}=\mathcal{H}_{\text{iso exch}}+\mathcal{H}_{\text{anti exch}}+\mathcal{H}_{\text{aniso}}, \tag{1}$$

where for the present we need consider explicitly only

$$\mathcal{H}_{\text{iso exch}}=-\sum_{ll'kk'}J_{lk,l'k'}\times\vec{s}_{lk}\cdot\vec{s}_{l'k'}.$$

s_{lk} refers to the spin on the *k*th iron sublattice in the *l*th unit cell. $\mathcal{H}_{\text{iso exch}}$ is the familiar isotropic Heisenberg exchange with a range as yet unspecified, $\mathcal{H}_{\text{anti exch}}$ the Dzyaloshinskii-Moriya antisymmetric exchange which is probably of importance only for nearest neighbors and is nonetheless smaller by $\sim 10^{-2}$ than the largest isotropic exchange terms. The single-ion anisotropy terms are smaller still, but it is the temperature dependence of the anisotropy which is responsible for the spin reorientation.

The inelastic-neutron-scattering intensity due to one-magnon scattering is proportional to the scattering function $S(\vec{Q},\omega)$, which can be written in the form[20]

$$S(\vec{Q},\omega)=[1+n(\omega)]\times\sum_{\alpha\beta}(\delta_{\alpha\beta}-Q_\alpha Q_\beta/|Q|^2)T_{\alpha\beta}(\vec{Q},\omega), \tag{2}$$

where $n(\omega)$ is the Bose thermal occupation factor, and

$$T_{\alpha\beta}(\vec{Q},\omega)=\sum_{kk'}F_k^*(\vec{Q})F_{k'}(\vec{Q})\times\operatorname{Im}\chi_{kk'}^{\alpha\beta}(\vec{Q},\omega). \tag{3}$$

Here the structure factor

$$F_k(\vec{Q})=f_k(\vec{Q})e^{i\vec{Q}\cdot\vec{R}_k},$$

$f_k(\vec{Q})$ being the form factor for the spin density of an ion on the *k*th sublattice, and $\chi_{kk'}(\vec{Q},\omega)$ is linear interlattice susceptibility, i.e.,

$$\delta\vec{s}(\vec{Q},\omega)=\chi_{kk'}(\vec{Q},\omega)\vec{h}_{k'}(\vec{Q},\omega),$$

where $\delta\vec{s}_k(\vec{Q},\omega)$ is the space-time Fourier transform of a spin fluctuation on the *k*th sublattice and $\vec{h}_k(\vec{Q},\omega)$ is the conjugate staggered magnetic field. $\chi_{kk'}(\vec{Q},\omega)$ has translational invariance in reciprocal space

$$\chi_{kk'}(\vec{Q},\omega)=\chi_{kk'}(\vec{q},\omega),$$

where $\vec{q}=\vec{Q}-\vec{G}$ lies in the first Brillouin zone. The poles of $\chi_{kk'}(\vec{q},\omega)$ are independent of kk' and coincide with the spin-wave frequencies. Equation (2) shows all four sublattice interactions are important for an understanding of the neutron-scattering results at a general $\vec{Q}$. This becomes rather cumbersome using the full Hamiltonian given in Eq. (1) and fortunately it is not necessary for the interpretation of the present experiments, because the general features of the spin-wave dispersion at high energy is determined by $\mathcal{H}_{\text{iso exch}}$ and the much smaller splittings due to the remaining terms are not observed. Section III is therefore concerned

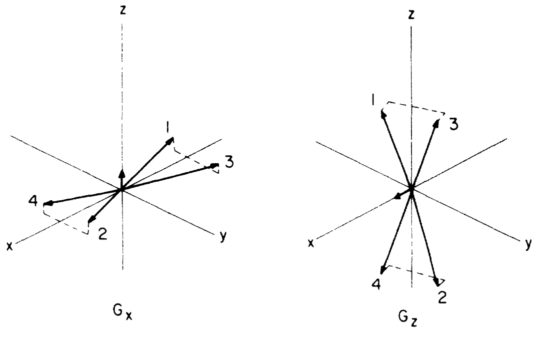

FIG. 2. Two allowed spin configurations in the orthoferrites. G_x, the high-temperature configuration, has the spins aligned along the *x* axis with a weak ferromagnetic moment along *z*. The low-temperature configuration G_z has the spins aligned along *z*, with a weak ferromagnetic moment along *x*.

with the interpretation of the gross (high-frequency) spin-wave dispersion using a full four-sublattice model and $\mathcal{H} = \mathcal{H}_{\text{iso exch}}$.

In Section IV the behavior of the low-energy spin waves, particularly at temperatures near the spin reorientation, are studied. It is then vital to use the full Hamiltonian, the consequences of which have been most extensively studied for two-sublattice models obtained by considering only the motion of the composite variables

$$\delta\vec{S}_{l1} = (\delta\vec{s}_{l1} + \delta\vec{s}_{l3})$$

and[21]

$$\delta\vec{S}_{l2} = (\delta\vec{s}_{l2} + \delta\vec{s}_{l4}).$$

The problem of discussing neutron-scattering results in RE FeO_3 by a two-sublattice model is somewhat more complex than for measurements of macroscopic quantities, e.g., in microwave-resonance experiments. The following is a discussion of the extent to which a simplification is possible. Define a new set of spin variables $\delta\vec{s}_{l\lambda}$ by a unitary transformation on $\delta\vec{s}_{lk}$,

$$\delta\vec{s}_{l\lambda} = U_{\lambda k}\delta\vec{s}_{lk} \quad (\lambda = O, P, Q, R).$$

Specifically (suppressing the l index),

$$\begin{aligned}
\delta\vec{s}_O &= \tfrac{1}{2}(\delta\vec{s}_1 + \delta\vec{s}_2 + \delta\vec{s}_3 + \delta\vec{s}_4) \\
&= \tfrac{1}{2}(\delta\vec{S}_1 + \delta\vec{S}_2), \\
\delta\vec{s}_P &= \tfrac{1}{2}(\delta\vec{s}_1 + \delta\vec{s}_2 - \delta\vec{s}_3 - \delta\vec{s}_4), \\
\delta\vec{s}_Q &= \tfrac{1}{2}(\delta\vec{s}_1 - \delta\vec{s}_2 + \delta\vec{s}_3 - \delta\vec{s}_4) \\
&= \tfrac{1}{2}(\delta\vec{S}_1 - \delta\vec{S}_2), \\
\delta\vec{s}_R &= \tfrac{1}{2}(\delta\vec{s}_1 - \delta\vec{s}_2 - \delta\vec{s}_3 + \delta\vec{s}_4).
\end{aligned}$$

Notice that the variables $\delta\vec{s}_P$ and $\delta\vec{s}_R$ cannot be expressed in terms of the "two-sublattice" variables. Making the same transformation of variables on Eq. (3) gives

$$T_{\alpha\beta}(\vec{Q}, \omega) = \sum_{\lambda,\lambda'} F^*_\lambda(\vec{Q}) F_{\lambda'}(\vec{Q})\, \mathrm{Im}\chi^{\alpha\beta}_{\lambda\lambda'}(\vec{Q}, \omega),$$

where $F_\lambda(\vec{Q}) = U_{\lambda k}F_k(\vec{Q})$, etc. With this representation a remarkable simplification occurs at reciprocal-lattice points, i.e., when $\vec{Q} = \vec{G} \equiv (h, k, l)$, namely, that one and only one structure factor $F_\lambda(G)$ is nonzero. We can therefore classify all reciprocal-lattice points by a label O, P, Q, R according to whether F_O, F_P, F_Q, or F_R is nonzero. The classification is shown in Table I. [Table I is written for the high-temperature RE FeO_3 structure (the G_x configuration of Fig. 2). It applies to the low-temperature (G_z) form by interchanging H and L components.] In studying long-wavelength magnetic fluctuations, the reciprocal-lattice vectors about which the observations are performed thus divide into two categories: (i) P- and R-type reflections which involve fluctuations that *cannot* be treated within the context of a two-spin model. These are the high-frequency "exchange" modes which are adequately treated by $\mathcal{H} = \mathcal{H}_{\text{iso exch}}$. (ii) O- and Q-type reflections which involve the low-lying "antiferromagnetic" modes which are describable with a two-spin formalism. These modes have zero frequency in the absence of anisotropy.

TABLE I. Classification of reciprocal-lattice points for the high-temperature RE FeO_3 structure.

Reflection type	(hkl)
O	(even, even, even), (odd, odd, even)
P	(odd, even, even), (even, odd, even)
Q	(odd, even, odd), (even, odd, odd)
R	(even, even, odd), (odd, odd, odd)

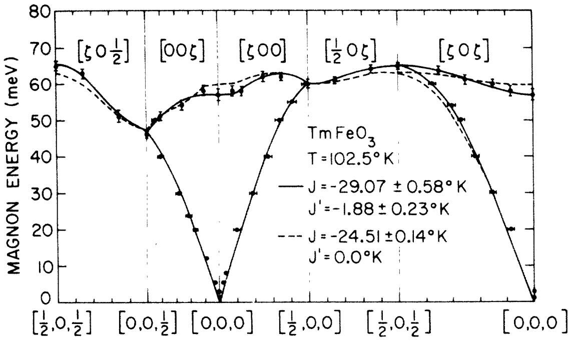

FIG. 3. Magnon dispersion curve along several symmetry directions in $TmFeO_3$ in the G_x configuration. The fits to the data with only nn exchange (dotted line) and with nn and nnn exchange (solid line) are also shown.

II. EXPERIMENTAL

The single crystals of $TmFeO_3$ and $ErFeO_3$ were grown at Bell Laboratories by the flux method described previously.[22] The $TmFeO_3$ crystal was plateletlike with dimensions $12 \times 15 \times 4$ mm^3 and the c axis perpendicular to the plate. The $ErFeO_3$ crystal was considerably smaller and approximately cubic in shape with a 5-mm edge size. The measured sample mosaics were 0.2° for $ErFeO_3$ and 0.3° for $TmFeO_3$. The majority of the measurements were performed in the $(h0l)$ scattering plane, but a study at several temperatures of the $\vec{q} = 0$ magnons in the $(0kl)$ scattering plane showed an identical behavior of the frequencies with temperature. The crystals were mounted in a temperature-controlled Dewar and the temperature regulated to better than 0.02 °K.

The neutron-scattering measurements were made on a triple-axis spectrometer at the Brookhaven high flux beam reactor. For the high-energy spin-wave dispersion measurements, we used an incident neutron energy (E_0) of 100, 110, 116, or 126 meV provided by the (110) reflection of a single-crystal beryllium monochromator. The scattered neutron energy was analyzed by the (002) reflection of another Be crystal. A Soller slit system with 40′ horizontal divergence was used to define the neutron path. The vertical divergence, determined by the natural collimator heights and the size of the crystals was approximately 2.0°. Both constant-Q and constant-E modes of operation were employed.

For the lower-energy magnons and the study of their behavior in the reorientation region, we used incident neutron energies of 13.5 and 4.9 meV. The monochromator was a bent pyrolytic graphite (PG) crystal and the analyzer was a flat PG crystal. Higher-order contamination of the incident neutron beam was reduced by a PG filter[23] at 13.7 meV and a polycrystalline beryllium filter[24] at 4.9 meV.

III. SHORT-WAVELENGTH SPIN-WAVE DISPERSION

The measured spin-wave dispersion at $T = 102.5\,^\circ\mathrm{K}$ along several symmetry directions in $\mathrm{TmFeO_3}$ is shown in Fig. 3. The sample was oriented to give an ($h0l$) scattering plane. The vertical error bars indicate the result of "constant-Q" scans, and the horizontal error bars denote data obtained by "constant-energy" scans. In accordance with the discussion in Sec. I, the data were fit using a four-sublattice model having only isotropic Heisenberg exchange with nn and nnn exchange constants (Fig. 1), which we denote as J and J', respectively. The spin-wave spectrum consists of two doubly degenerate branches with eigenvalues given by[25]

$$(\hbar\omega)^2_\pm = (A \pm C)^2 - (B \pm D)^2, \tag{4}$$

where

$$\begin{aligned} A &= 2S\{2[-3J + J'(6 - \cos\theta_x \\ &\qquad - \cos\theta_y)]\}, \\ B &= -2S(2J\cos\theta'_z), \\ C &= -2S(8J'\cos\theta'_x\cos\theta'_y\cos\theta'_z), \\ D &= -2S(4J\cos\theta'_x\cos\theta'_y), \end{aligned}$$

with

$$\begin{aligned} &\theta_x = q_x a = 2\pi\zeta_x, \quad \theta_y = q_y b = 2\pi\zeta_y, \\ &\theta'_x = \tfrac{1}{2}q_x a = \pi\zeta_x, \quad \theta'_y = \tfrac{1}{2}q_y b = \pi\zeta_y, \\ &\theta'_z = \tfrac{1}{2}q_z c = \pi\zeta_z. \end{aligned}$$

The solid curve in Fig. 3 shows the best least square fit to the data which were obtained by setting $J_{12} = J_{24} = J = -29.1(\pm 0.6)\,^\circ\mathrm{K}$ and $J_{11} = J_{13} = J' = -1.9(\pm 0.2)\,^\circ\mathrm{K}$. For comparison, the dotted curve is the best-fitting solution allowing only nn exchange. In reality, the nearest-neighbor exchange constants are distinct by virtue of the distortion from cubic symmetry, and there are also two nnn constants, but attempts to refine these four parameters separately produced nearly identical exchange constants without a statistically significant improvement in fit. This is consistent with structural information[26] which shows that Fe-O-Fe angles and distances and thus the superexchange paths are nearly identical for the two types of nn configurations. Similar results are obtained for nnn configurations.

The negative (antiferromagnetic) nn exchange is predicted by the Goodenough-Kanamori (GK) rules and the magnitude is in reasonable agreement with that deduced from the value of the Néel temperature (T_N) using mean-field theory.[27] The measurements suggest that J' is approximately $\frac{1}{15}$ of J and also antiferromagnetic. The only other reliable estimates of nnn exchange in perovskites come from studies of the magnetic properties of ordered binary compounds $AB(\mathrm{I})\mathrm{O_3} - AB(\mathrm{II})\mathrm{O_3}$, where B(II) is diamagnetic and the structure is so arranged that the magnetic B(I) ions occupy nnn sites.[28] The materials order with $T_N \sim 20$ times smaller than the pure $AB(\mathrm{I})\mathrm{O_3}$, implying values of J'/J consistent with our estimate.

Notice that although J' is antiferromagnetic, nnn nonetheless have spins parallel, since to be otherwise would necessitate the breaking up of some nn antiparallel couplings. Thus although the spin arrangement in Fig. 1 represents the ground state as $J'/J \to 0$, it is clear that in the opposite limit, some other ground state exists. This has been studied in mean-field theory by Ter Haar and Lines[29] who showed that the configuration of Fig. 1 is stable as long as $J \geq 4J'$, which is easily satisfied in the present case.

IV. LONG-WAVELENGTH SPIN WAVES AND SPIN REORIENTATION

The spin-reorientation phenomenon is always discussed in the long-wavelength limit of the two-sublattice model. That is, it is assumed that the relevant variables are the $\vec{q} = 0$ components of the normalized composite spin variables

$$\vec{S}^0_1 = (1/2S)(\vec{s}^0_1 + \vec{s}^0_3)$$

and

$$\vec{S}^0_2 = (1/2S)(\vec{s}^0_2 + \vec{s}^0_4).$$

The magnitude of the spin of a single Fe^{3+} ion is $S = \frac{5}{2}$. In particular, the term $\mathcal{H}_{\mathrm{aniso}}$ in Eq. (1) may be written[21,30]

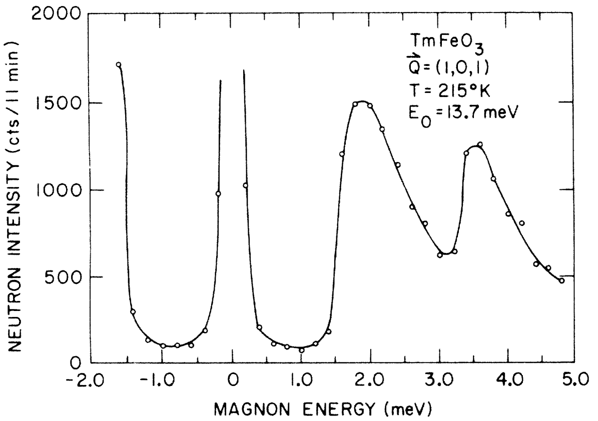

FIG. 4. Low-frequency $q=0$ spin-wave spectrum for $\mathrm{TmFeO_3}$.

$$\mathcal{H}_{\mathrm{aniso}} = -\sum_{k=1,2} [A_{xx}(S^0_{kx})^2 + A_{zz}(S^0_{kz})^2] + 2K_4 \sum_{\substack{k=1,2\\ i=x,y,z}} (S^0_{ki})^4. \tag{5}$$

In both $\mathrm{TmFeO_3}$ and $\mathrm{ErFeO_3}$ the spin reorientation occurs near 90 °K with $T_u - T_l \sim 10$ °K. Both Mössbauer[31] and neutron diffraction[5] studies have shown the reorientation to occur by a smoothly continuous coherent rotation of all the spins. Horner and Varma[32] showed that this behavior could be understood using a free energy of the form

$$F(T) = F_0 + \tfrac{1}{2}K_2(T)\cos 2\theta + K_4 \cos 4\theta, \tag{6}$$

where θ is the angle between the z axis and the weak ferromagnetic moment and $K_2(T) = -2(A_{xx} - A_{zz})$. Levinson *et al.*[33] showed that this free energy could be derived from a Hamiltonian of the form of Eqs. (1) and (5) by thermodynamic perturbation theory to lowest order in (anisotropy energy/exchange energy). Applying equilibrium conditions to Eq. (6) we find three distinct temperature regions, distinguished by the value of θ:

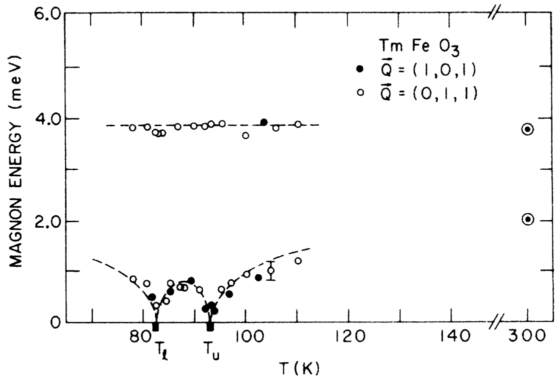

FIG. 6. Magnon energy vs temperature for $q=0$ spin waves in $\mathrm{TmFeO_3}$. The solid curve is calculated from Eqs. (7) and the parameters given in Table II.

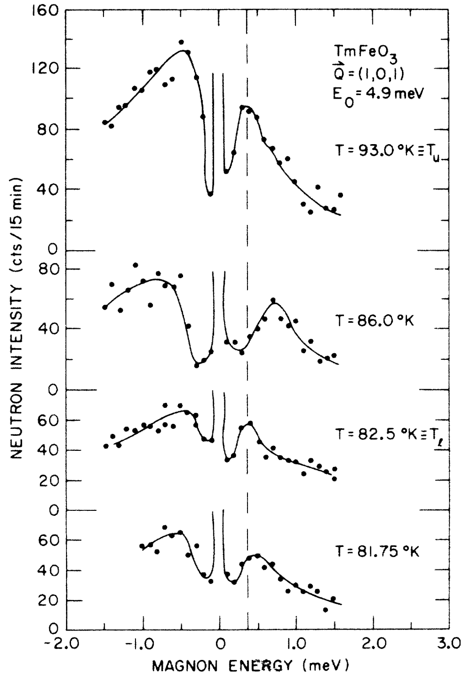

FIG. 5. High-resolution low-frequency $q=0$ spin-wave spectra of $\mathrm{TmFeO_3}$ exhibiting the renormalization of the low-frequency magnons with temperature. The dotted line is the value of the frequency at T_u and T_l.

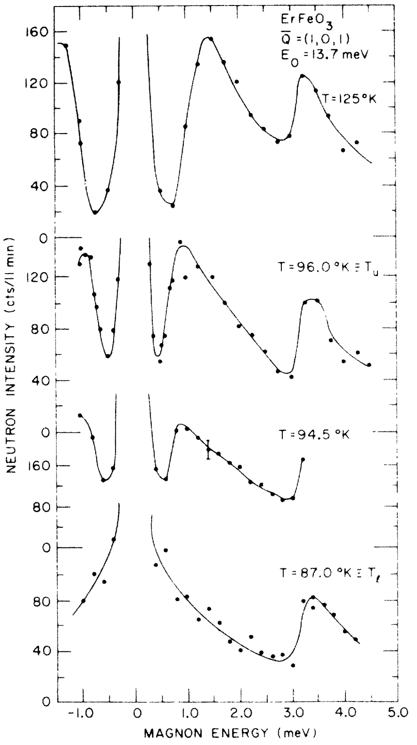

FIG. 7. Spin-wave spectra in $\mathrm{ErFeO_3}$ at several temperatures.

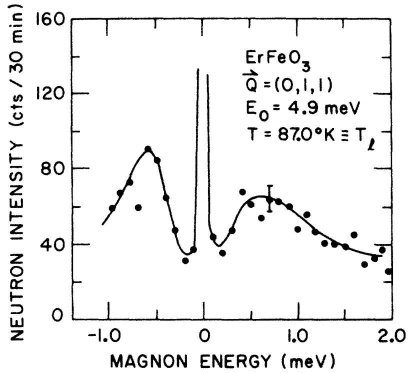

FIG. 8. High-resolution $q=0$ spin-wave spectrum of $\mathrm{ErFeO_3}$ at $T=T_l$.

I: $\theta=0,\quad T\geq T_u$

II: $\theta=\frac{1}{2}\pi\quad T\leq T_l,$

III: $\cos 2\theta=-K_2(T)/8K_4,\quad T_l\leq T\leq T_u$

with T_u and T_l determined by the conditions $K_2(T_u)=-8K_4$ and $K_2(T_l)=8K_4$.

The spin reorientation is on this basis expected to show two second-order transformations at T_u and T_l with order parameters θ and $\frac{1}{2}\pi-\theta$, respectively. The temperature dependence of θ in the "ordered" phase (III) is determined by $K_2(T)$ which was shown to vary approximately linearly with temperature in $\mathrm{SmFeO_3}$,[34] the only orthoferrite in which it has been measured.

$\mathcal{H}_{\text{aniso}}$, in addition to determining the ground state of the system by removing the rotational degeneracy, causes an energy gap (in fact a pair of them) to appear in the $\vec{q}=0$ "antiferromagnetic" spin-wave branches. The frequencies of the two low-lying $\vec{q}=0$ spin-wave branches are given approximately by[18,19,30]

TABLE II. Reorientation temperatures, exchange, and anisotropy energies for $\mathrm{TmFeO_3}$ and $\mathrm{ErFeO_3}$. (For conversion into energy density, $1\,^\circ\mathrm{K}\approx 0.62\times10^6\ \mathrm{erg/cm^3}$).

(°K)	$\mathrm{TmFeO_3}$	$\mathrm{ErFeO_3}$
T_u	92.8 (±1)	95.8 (±0.5)
T_l	82.5 (±0.5)	87.3 (±1)
E	4370 (±90)	
K_0	2.33 (±0.15)	
K_2	4.2 (±1) $(1-1.14\times10^{-2}T)$	
K_4	3.1 (±0.7)$\times10^{-2}$	

$$(\hbar\omega_1)^2=[4E/2S)^2](-\tfrac{1}{2}K_2\cos 2\theta-4K_4\cos 4\theta),$$
$$(\hbar\omega_2)^2=[4E/(2S)^2](K_0-\tfrac{1}{4}K_2\cos 2\theta-K_4\cos 4\theta),\qquad(7)$$

where $K_0=\frac{1}{2}(A_{xx}+A_{zz})$ and $E=-6J(2S)^2$ is the effective two-sublattice exchange constant. Equation (7) has been simplified by again dropping terms smaller by the order (anisotropy energy/exchange energy). Note, however, that the relations determining T_u and T_l are such that $\omega_1^2\rightarrow 0$ at T_u and T_l. Thus the dynamical instability which is inferred by the vanishing of the force conjugate to θ, $-\partial^2F/\partial\theta^2$, is manifested as a "soft-mode" behavior in one of the $\vec{q}=0$ "antiferromagnetic" spin waves. The "soft" mode with frequency ω_1 has large fluctuations in the x-z plane,[21] whereas the remaining mode, with a large y component of spin precession is predicted to stay nearly temperature independent throughout the spin reorientation.

Figure 4 shows the inelastic magnetic scattering about the (1, 0, 1) reciprocal-lattice vector, which is suitable (Q type) for studying the low-lying "antiferromagnetic" modes, at a temperature far above the reorientation region. As expected, two $\vec{q}=0$

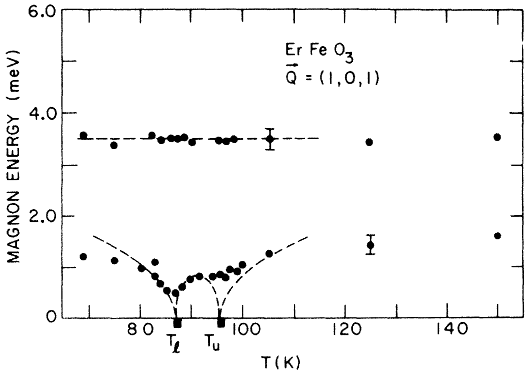

FIG. 9. Magnon energy vs temperature for $q=0$ spin waves in $\mathrm{ErFeO_3}$. The solid curve is calculated from Eqs. (7) using parameters similar to those in Table II.

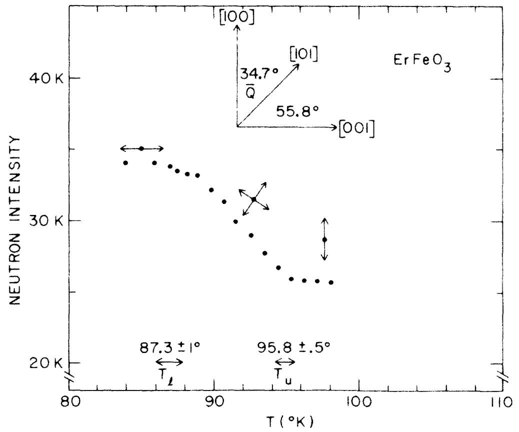

FIG. 10. Intensity of neutrons Bragg reflected from (101) reciprocal-lattice point in $\mathrm{ErFeO_3}$ vs temperature. Inset shows the angles between $\vec{Q}_{(101)}$ and the x and z axis.

modes are observed. The magnon groups are asymmetric toward higher energy due principally to the interaction of the finite spectrometer $\vec{Q}$ resolution with the rather steep magnon dispersion.[35] The true $\vec{q} = 0$ frequency thus corresponds more nearly to the maximum than to the center of gravity of the observed scattering. This is moderately high-resolution data taken with an incident neutron energy of 13.7 meV. Figure 5 is a representative sample of higher-resolution data taken in the reorientation region. The results of all such measurements are shown in Fig. 6. It is clear that the lowest-lying mode is indeed "soft" and in qualitative agreement with theory, showing pronounced frequency minima near T_u and T_l. The higher-frequency mode is essentially temperature independent, again in agreement with theoretical expectation. It is clear, however, that the soft-mode frequency does not go to zero but remains finite at both transformation temperatures.

The situation is much less satisfactory in $ErFeO_3$ as Fig. 7 demonstrates. Well above the reorientation region, the spectrum closely resembles that of $TmFeO_3$. However, the frequency renormalization is much less in the region just above T_u, but continues to decrease between T_u and T_l, until at T_l it is sufficiently low to be completely masked by the strong Bragg scattering when observed with moderate resolution. But higher-resolution measurements, Fig. 8, makes it clear that $\omega_1(T_l)$ is still finite. The data for $ErFeO_3$ are summarized in Fig. 9, which is similar to Fig. 6 for $TmFeO_3$ except at T_u where there is almost no dip in $\omega_1(T)$.

It is straightforward using the data of Fig. 6 and Eqs. (7) to estimate the various parameters in $\mathcal{H}_{\text{aniso}}$ for $TmFeO_3$. If K_4 is assumed temperature independent and K_2 is written as $K_2(T) = a - bT$, K_4 is determined from ω_1 at the midpoint of the reorientation region where $K_2(T) = 0$. A knowledge of K_4 and the width of the reorientation region then suffices to determine $K_2(T)$. Finally, the upper-branch frequency can be used to determine K_0 which is also assumed to be temperature independent. The values obtained for $TmFeO_3$ are shown in Table II, and the calculated temperature-dependent frequencies are shown in Figs. 6 and 9. The values for the anisotropy energy are roughly an order of magnitude larger than those measured in $SmFeO_3$.[34] These same $SmFeO_3$ values were assumed for $ErFeO_3$ by Gorodetsky and Lüthi (GL).[18] It is clear from Fig. 6 that the assumed linear temperature dependence for $K_2(T)$ is not satisfactory over a large temperature range.

We have investigated the possibility that the failure of the soft mode in $TmFeO_3$ to vanish at both T_u or T_l is the result of magnetoelastic coupling. The consequences of this coupling on the elastic response of $ErFeO_3$ has been examined in detail by GL,[18] who show that coupling with the elastic constant C_{55} does prevent the soft-mode frequency from vanishing at T_u and T_l. However, a quantitative estimate of the effect shows that magnetoelastic coupling constants much larger ($B_{55} \sim 1.5 \times 10^8$ erg/cm^3) than suggested by GL for $ErFeO_3$,[18] and possibly unrealistically large,[36] would be necessary to account for our observations in this manner. It seems somewhat more plausible to ascribe the saturation of the soft mode in $TmFeO_3$ to sample inhomogeneity. A spread of ±1° in the transformation temperatures would be sufficient to produce this effect. We cannot, however, exclude the possibility of some more complicated behavior involving a saturation of the "soft" sidebands together with the appearance of a divergent quasielastic peak. Such behavior has recently been observed in several structural phase transformations.[37]

In an effort to understand the peculiar asymmetry in the behavior of $ErFeO_3$ about T_u and T_l intensity measurements were performed on the (101) magnetic Bragg reflection at various temperatures as shown in Fig. 10. It is possible to sense the spin reorientation in this way since the scattering intensity is proportional to $\sin^2\phi$ where ϕ is the angle between the scattering vector $\vec{Q}$ and the spin direction. As can be seen from the inset in Fig. 10, ϕ decreases as the spins rotate from the x to the z directions. The values of T_u and T_l obtained in this way are reasonably well defined and in agreement with those obtained by other methods.[16,17,18] Furthermore, samples from the same growth batch show pronounced ultrasonic velocity anomalies at temperatures equal to those obtained from Fig. 10.[38] It does not therefore appear possible to account for the small degree of mode softening at T_u by inhomogeneity in the transformation temperature. In fact, we can offer no satisfactory explanation of this behavior at the present time, and for this reason it does not seem profitable to analyze the existing data for $ErFeO_3$ to obtain anisotropy parameters.

ACKNOWLEDGMENTS

We thank D. E. Cox and B. Lüthi for valuable discussions.

---

*Work performed under the auspices of the U. S. Atomic Energy Commission.

[1] A review of the properties of rare-earth orthoferrites is given by R. L. White, J. Appl. Phys. 40, 1061 (1969).

[2] See, for example, W. Cochran, Adv. Phys. 18, 157 (1969).

[3] S. Geller and E. Wood, Acta Crystallogr. 9, 563

(1956); M. Marezio, J. P. Remeika, and P. D. Dernier, Acta Crystallogr. B 26, 300 (1970).

[4] W. C. Koehler, E. O. Wollan, and M. K. Wilkinson, Phys. Rev. 118, 58 (1960).

[5] J. A. Leake, G. Shirane, and J. P. Remeika, Solid State Commun. 6, 15 (1968).

[6] E. F. Bertaut, in *Magnetism*, edited by G. T. Rado and H. Suhl (Academic, New York. 1963), Vol. III, p. 149.

[7] I. E. Dzyaloshinskii, J. Phys. Chem. Solids 4, 241 (1955).

[8] T. Moriya, Phys. Rev. 156, 562 (1967).

[9] D. Treves, Phys. Rev. 125, 1843 (1962); G. Gorodetsky and D. Treves, Phys. Rev. 135, A97 (1964).

[10] E. M. Gyorgy, J. P. Remeika, and F. B. Hagedorn, J. Appl. Phys. 39, 1369 (1968).

[11] M. Eibschütz, S. Shtrikman, and D. Treves, Phys. Rev. 156, 562 (1967).

[12] R. W. Grant and S. Geller, Solid State Commun. 7, 1291 (1969).

[13] D. L. Wood, L. M. Holmes, and J. P. Remeika, Phys. Rev. 185, 689 (1969).

[14] K. B. Aring and A. J. Sievers, J. Appl. Phys. 41, 1197 (1970).

[15] A. P. Malozemoff, J. Phys. Chem. Solids 32, 1669 (1971).

[16] H. Pinto, G. Shachar, H. Shaked, and S. Shtrikman, Phys. Rev. B 3, 3861 (1971).

[17] R. C. LeCraw, R. Wolfe, E. M. Gyorgy, F. B. Hagedorn, T. C. Hensel, and J. P. Remeika, J. Appl. Phys. 39, 1019 (1968).

[18] G. Gorodetsky and B. Lüthi, Phys. Rev. B 2, 3688 (1970).

[19] G. F. Herrmann, Phys. Rev. 133, A1334 (1964).

[20] See, for example, W. Marshall and S. W. Lovesey, *Theory of Thermal Neutron Scattering* (Oxford U. P., Oxford, 1971).

[21] G. F. Herrmann, J. Phys. Chem. Solids 24, 597 (1963).

[22] J. P. Remeika and T. Y. Kimetani, Mater. Res. Bull. 3, 895 (1968).

[23] G. Shirane and V. J. Minkiewicz, Nucl. Instrum. Methods 89, 109 (1970).

[24] B. N. Brockhouse, in *Inelastic Scattering of Neutrons in Solids and Liquids* (IAEA, Vienna, 1961), p. 113.

[25] E. J. Samuelsen, Physica 43, 353 (1969).

[26] M. Marezio, J. P. Remeika, and P. D. Dernier, Acta Crystallogr. B 26, 2008 (1970).

[27] J. S. Smart, in *Magnetism*, edited by G. T. Rado and H. Suhl (Academic, New York, 1963), Vol. III, p. 63.

[28] G. Blasse, J. Appl. Phys. 36, 879 (1965).

[29] D. Ter Haar and M. E. Lines, Philos. Trans. R. Soc. Lond. A 254, 521 (1962).

[30] J. R. Shane, Phys. Rev. Lett. 20, 728 (1968).

[31] G. Gorodetsky, L. M. Levinson, S. Shtrikman, D. Treves, and B. M. Wanklyn, Phys. Rev. 187, 637 (1967).

[32] H. Horner and C. M. Varma, Phys. Rev. Lett. 20, 845 (1968). They present equivalent results with $\sin^2\theta$ and $\sin^4\theta$ terms with appropriately defined coefficients.

[33] L. M. Levinson, M. Luban, and S. Shtrikman, Phys. Rev. 187, 715 (1969). These authors also consider anisotropic exchange terms and show that they do not change the form of $F(T)$.

[34] K. P. Belov, R. A. Volkov, B. P. Goranskii, A. M. Kadomtseva, and V. V. Uskov, Fiz. Tverd. Tela 11, 1148 (1969) [Sov. Phys.-Solid State 11, 935 (1969)].

[35] E. J. Samuelsen, M. T. Hutchings, and G. Shirane, Physica 48, 13 (1970).

[36] W. I. Dobrov, Phys. Rev. 134, A734 (1964).

[37] See, for example, J. D. Axe, S. M. Shapiro, G. Shirane, and T. Riste, in *Anharmonic Lattices, Structural Transformations and Melting*, edited by T. Riste (Noordhof, Leiden, 1974), p. 23.

[38] B. Lüthi (private communication).